245 GHz High-Field EPR Study of Tyrosine-D° and Tyrosine-Z° in Mutants of Photosystem II†

Sun Un,*,‡ Xiao-Song Tang,§ and Bruce A. Diner§

Section de Bioénergétique, URA1290 CNRS, Deptartment Biologie Cellulaire et Moléculaire, CEA-Saclay, F-91191 Gif-sur-Yvette, France, Central Research and Development Department, Experimental Station, E. I. Du Pont de Nemours & Co., Wilmington, Delaware, 19880-0173

Received October 4, 1995; Revised Manuscript Received November 27, 1995⊗

ABSTRACT: A 245 GHz 8.7 T high-field EPR study of tyrosine-D (TyrD°) and tyrosine-Z (TyrZ°) radicals of photosystem II (PSII) from *Synechocystis* PCC 6803 was carried out. Identical principal *g* values for the wild-type *Synechocystis* and spinach TyrD° showed that the two radicals were in similiar electrostatic environments. By contrast, the principal *g* values of the TyrD° in the D2-His189Gln mutant of *Synechocystis* were different from those of the wild-type and spinach radicals and were similar to those of the tyrosyl radical in ribonucleotide reductase. These comparisons indicate that the D2-His189Gln mutant TyrD° is not hydrogen-bonded or is only weakly so. The HF-EPR spectrum of TyrZ° was obtained from the D2-Tyr160Phe mutant that lacks TyrD°. The principal *g* values were nearly identical to those of the wild-type TyrD°. The low-field edge of the TyrZ° spectrum was much broader than at the other two principal *g* values and was also much broader than the TyrD° spectrum. From the identical *g* values and previous work on tyrosyl radical *g* values [Un S., Atta M., Fontecave, M., & Rutherford, A. W. (1995) *J. Am. Chem. Soc. 117*, 10713−10719], it was concluded that TyrZ° , like TyrD°, is hydrogen-bonded. The broadness of the g_x component was interpreted as a distribution in strength of the hydrogen-bonding due to disorder in the protein environment about TyrZ°.

Two unique tyrosine radicals are found in photosystem II (PSII),[1] known as tyrosine-D (TyrD°) and tyrosine-Z (TyrZ°). On the basis of the analogy to the known structure of the bacterial reaction center (Deisenhofer et al., 1985) and similarities in the primary structures of the bacteria reaction center and photosystem II subunits, these tyrosyl radicals are thought to occupy symmetry related positions within PSII (Michel & Deisenhofer, 1988; Vermaas et al., 1988; Debus et al., 1988a,b; Metz et al., 1989; Svenson et al., 1990, 1991; Ruffle et al., 1992). Recent distance measurements using saturation−recovery EPR (Koulougliotis et al., 1995) show that TyrZ° and TyrD° are equidistant from the non-heme iron providing support for symmetric placement of these radicals in PSII. Paradoxically, this symmetry does not extend to their chemical state and function. TyrD° is a stable radical [for example, see Babcock et al. 1989)] and does not play a known role in the normal electron transfer reaction. By contrast, the TyrZ° is short lived and is an active electron transport component. Among other factors, the radical lifetime depends on the state of the manganese cluster within PSII (Babcock et al., 1976; Dekker, 1984). The differences in hydrogen-bonding state of the tyrosyl radicals have been suggested to be an important discriminating factor (Tommos et al., 1995). Recently, cw and pulsed EPR together with ENDOR have been used extensively to probe possible differences in the radical themselves as well as their local environments [for example, see Tommos et al. (1995) and Tang et al. 1996)].

A relatively new alternative to conventional 9 GHz EPR is high-field EPR (HF-EPR).[1] This new technique is conceptually identical to the conventional one except that it utilizes magnetic fields large enough to resolve radicals by their *g* values. Equally important, at high fields, the anisotropy in the *g* values can be measured. In the present work, we report HF-EPR results obtained using a magnetic field of 8.7 T and a microwave frequency of 245 GHz. It has been shown previously (Un et al., 1995) and will be further demonstrated in this paper that the *g* values of tyrosyl radicals carry detailed information regarding their chemical environments. The factors which influence *g* values of tyrosyl radicals have been identified using quantum mechanical arguments and semiempirical molecular orbital calculations (Un et al., 1995). Qualitatively, the results may be summarized as follows: (a) the g_z component (ring perpendicular direction) is smaller than the free electron *g* values (Stone, 1963; Angstl, 1989) but is approximately constant for all tyrosyl radicals with a value of approximately 2.00212 (Figure 1); (b) the g_x component (the C−O direction) is very sensitive to the electrostatic stabilization of the nonbonding oxygen electrons by the protein with values extending from 2.0064 for strongly hydrogen-bonded or electrostatically stabilized situations to 2.0090 for neutral environments; (c) the g_y component is relatively insensitive to environmental effects and has an approximate value of 2.0045. Specifically, it was concluded that the g_x component of the ribonucleotide reductase (RNR) tyrosyl radical spectrum was determined by electrostatic interactions between the tyrosyl radical and the nearby positively charged binuclear iron site and the

† This research was supported by a grant from the Human Frontiers Science Organization.

‡ CNRS.

§ E. I. Du Pont de Nemours & Co.

⊗ Abstract published in *Advance ACS Abstracts,* January 1, 1996.

[1] Abbreviations: EPR, electron paramagnetic resonance; HF-EPR, high-field electron paramagnetic resonance; MNDO, modified neglect of diatomic overlap; PM3, parametric method 3; SOMO, singly occupied molecular orbital; RNR, ribonucleotide reductase.

0006-2960/96/0435-679$12.00/0

negatively charged ligands of the irons. The net effect was a weak electrostatic stabilization of the nonbonding oxygen electrons leading to a g_x value of 2.0087. By contrast, for TyrD° in spinach photosystem II, the g_x value of 2.0075 was concluded to arise from the stabilization of the oxygen nonbonding electrons by a modest strength hydrogen bond. The presence of a hydrogen bond is consistent with 9 GHz ENDOR and ESEEM observations [Rodriguez et al. (1987) and Evelo et al. (1989), respectively]. This electrostatic model also correctly accounted for the *g* values of the *in vitro* tyrosyl radical (Fasanella & Gordy, 1969). This *in vitro* radical is more strongly hydrogen-bonded than TyrD° with a g_x value of 2.0064. As the electrostatic interaction between a donor and an acceptor plays a major role in hydrogen-bonding (Schuster, 1976; Pimentel & McClellan, 1960), the effect of a hydrogen bond on the g_x values of tyrosyl radicals is indistinguishable from any other electrostatic interactions. However, no positively charged amino acid side chain (i.e., lysine, arginine, histidine) can provide electrostatic stabilization and not be a potential hydrogen-bond donor. Therefore, if no positively charged non-amino acid groups are present, low g_x values, as that observed for TyrD°, indicate the proximity of one or more hydrogen-bond donor(s).

In this communication, we report results from our HF-EPR study of two mutants of PSII from *Synechocystis* PC6803, one (D2-His189Gln) in which the local environment about TyrD° has been modified and another (D2-Tyr160Phe) that lack TyrD°, but where the TyrZ° radical has been trapped. Histidine-189 of the D2 polypeptide of PSII has been identified as the hydrogen-bond donor to TyrD° (Tang et al., 1993). Hence, the D2-His189Gln mutant provides a convienent way to study the effects of hydrogen-bonding on TyrD° and on its *g* values. Using the theory that we have developed for tyrosyl radical *g* values, we draw some conclusions about the importance of the hydrogen-bonding and local electronic environment on the observed differences between TyrZ° and TyrD°.

MATERIALS AND METHODS

Mutants D2-Tyr160Phe and D2-His189Gln were constructed in the psbDI gene of the "olive" strain *Synechocystis* 6803 as previously described (Tang et al., 1993 and 1996, respectively). The presence and integrity of the mutated gene was verified by Southern hydrization and by direct sequencing of PCR amplified DNA in the region of the mutations.

Non-oxygen-evolving, manganese-depleted PSII core complexes were isolated from the mutant and wild-type strains of *Synechocystis* as previously described (Tang et al., 1996). The samples were suspended in 50 mM MES-NaOH, pH 6.0, containing 20 mM $CaCl_2$, 5 mM $MgCl_2$, 25% (w/v) glycerol, and 0.004% dodecyl maltoside, concentrated to ~2 mg of chlorophyll/mL in Centricon 100s (Amicon). Potassium ferricyanide was added to a final concentration of 0.3 mM. The samples were then loaded into EPR tubes.

For measurements of TyrD°, the samples were illuminated at 0 °C for 15−20 s using a tungsten light source (Model I-150, Cuda Products, Inc.) and then dark adapted on ice for 10 min prior to freezing and storage in liquid nitrogen. For measurements of TyrZ°, the samples were prepared as described previously (Tang et al., 1996).

The HF-EPR spectrometer has been previously described (Muller et al., 1989). The HF-EPR samples were frozen inside standard 3 mm quartz EPR tubes and placed into the magnet. The absolute uncertainty in *g* value measurements was estimated to be $\pm 2 \times 10^{-4}$. The large uncertainty results from systematic errors due to magnet-field calibration and control. For a given sample, the spectra were reproducible to within $\pm 2 \times 10^{-5}$ in terms of *g* values. Conventional 9 GHz EPR spectra of all the samples were obtained before and after the HF-EPR experiments using exactly the same sample and EPR tubes. No difference in the 9 GHz spectra was observed. All HF-EPR spectra were taken between 3 and 5 K with 10 G and 10 kHz modulation under nonsaturating conditions. The 9 GHz spectra were obtained at 10 K with 1.2 G and 100 kHz modulation under nonsaturating conditions.

The theoretical *g* value calculations discussed below are presented in detail in a separate work (Un et al., 1995).

RESULTS AND DISCUSSION

Wild-type TyrD°. Figure 1 shows the 245 GHz HF-EPR spectrum of the tyrosyl radicals from RNR, spinach Photosystem II, wild-type (WT), and two mutants of *Synechocystis*. Figure 2 shows the corresponding 9 GHz EPR spectra of the WT and the three mutants. The ribonucleotide reductase (RNR) and spinach photosystem II 245 GHz spectra have been discussed in detail in a previous report (Un et al., 1995) and are summarized above. The *g* values are given in Table 1. As expected, the principal *g* values of wild-type TyrD° (WT-TyrD°, Figure 1D) are identical to those of TyrD° in spinach (Figure 1E). From this, we conclude that TyrD° in the WT *Synechocystis* exists in the same electrostatic environment as in spinach. Specifically, the extent of hydrogen-bonding to the radical is the same in both. As in the case of spinach TyrD°, the overall shape of the WT-TyrD° spectrum is distorted and is similar to that found for spinach TyrD° in absence of the manganese cluster (Un et al., 1994). The PSII complexes discussed here also lack intact manganese clusters; hence, the distortion likely arises from anisotropic dipolar relaxation effects from the non-heme iron (Un et al., 1994) and possibly other nonspecific paramagnetic metals in the sample. The apparent line widths of the WT and spinach spectra at the principle *g* values (i.e., at the field positions corresponding to g_x, g_y, and g_z) are similiar. Since the line widths of the HF-EPR spectra are dominated by unresolved proton-hyperfine couplings, these couplings must be similar in both radicals. This is consistent with the 9 GHz EPR measurements which show that the hyperfine couplings are nearly identical for WT-TyrD° and spinach TyrD° (Tommos et al., 1993). For the RNR and spinach cases, the largest hyperfine coupling is due to the electron spin interaction with one of the β-methylene protons (i.e., protons adjacent to the phenyl ring). These β-methylene proton hyperfine couplings are also the most variable from one tyrosyl radical to another. This is because the magnitudes of the couplings depend on the relative orientation of the C_β-H bonds to the phenyl ring plane. The isotropic component of the β-methylene proton coupling is given by

$$A_{iso} \approx 21G \cos^2\theta \qquad (1)$$

where θ is the angle between the C_β-H and phenyl-ring plane normal (Heller & McConnell, 1960; Warncke et al., 1994). In the case of RNR, the dihedral angle is nearly 0° (Nordlund

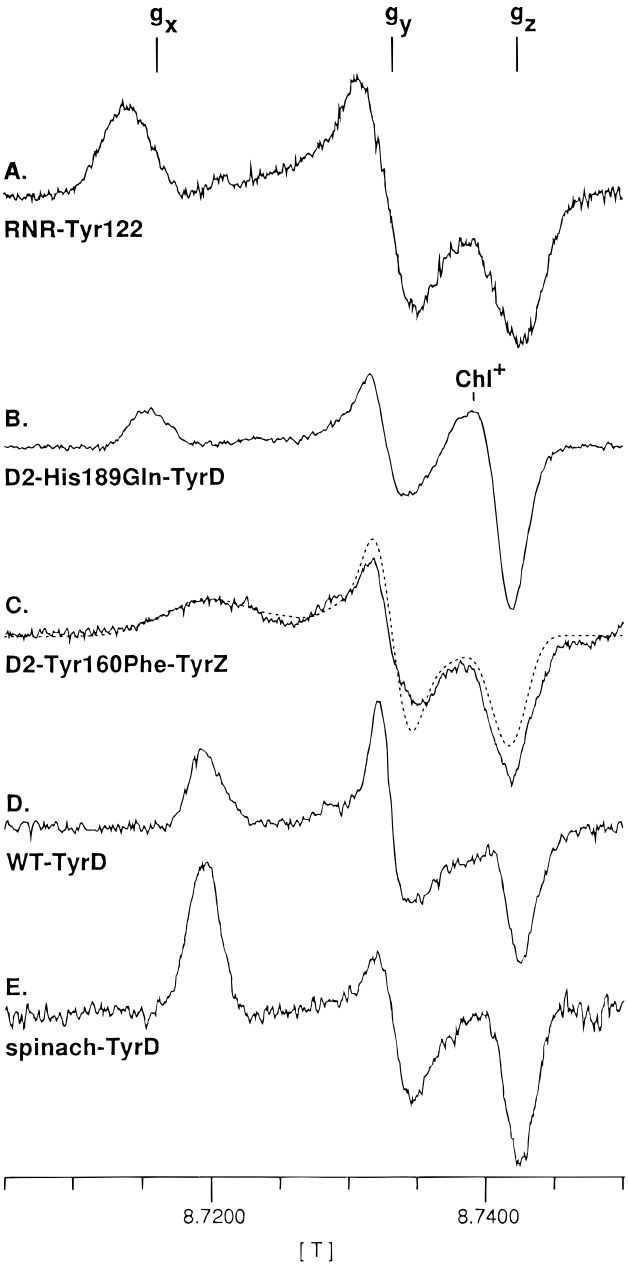

FIGURE 1: 245 GHz 8.7 T spectra of tyrosyl radicals: (A) Tyr122 in ribonucleotide reductase from *E. coli*. (B) TyrD° in the D2-His189Gln mutant. (C) TyrZ° in the D2-Tyr160Phe mutant and (D) TyrD° in wild-type *Synechocystis*. (E) TyrD° in spinach photosystem II. The calculated spectrum of TyrZ° based on the measured hyperfine coupling for TyrD° (Tommos, 1994) with a isotropic H(C_β) hyperfine coupling of 12 G and a Gaussian distribution in g_x of 0.0007 (see text for details) is shown sumperimposed on spectrum C (dotted lines). All spectra were obtained between 3.7 and 4.2 K with a modulation amplitude of 10 G and modulation frequency of 250 Hz for A and E and 10 kHz for B, C, and D. All spectra were obtained under nonsaturating conditions.

& Eklund, 1993) and the isotropic component of the coupling is about 20 G (Bender et al., 1989). For the spinach and WT cases, the angle is approximately 50° and the isotropic coupling approximately 8 G (Hoganson & Babcock, 1988; Rigby et al., 1994; Warncke et al., 1994; Tommos et al., 1994). Simulations (not shown) show that the larger line widths observed in the HF-EPR spectra of the RNR tyrosyl radical in comparison to TyrD° can be accounted for by this larger hyperfine coupling.

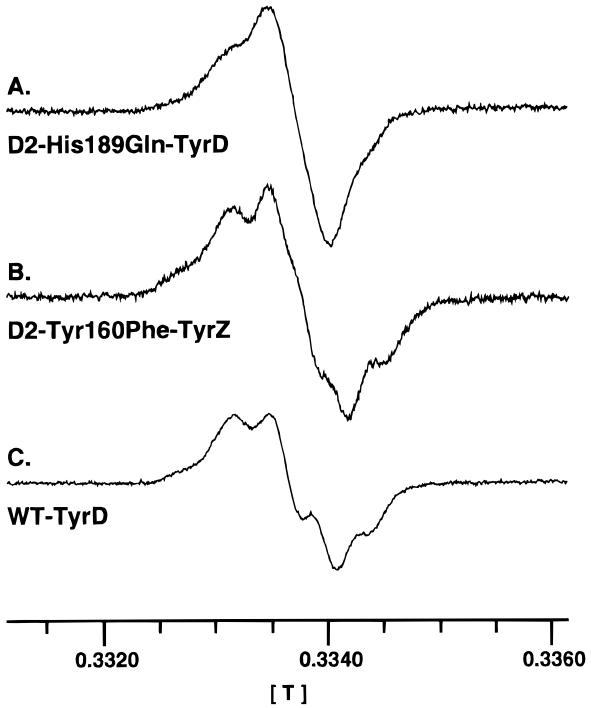

FIGURE 2: 9 GHz spectra of tyrosyl radical in isolated core complexes from *Synechocystis*. (A) TyrD° from the D2-His189Gln mutant. (B) TyrZ° from the D2-Tyr160Phe mutant. (C) TyrD° from wild-type. All spectra were obtained 10 K with a modulation amplitude of 1.2 G and frequency of 100 kHz. All spectra were obtained under nonsaturating conditions.

Table 1: The *g* Values of Tyrosyl Radicals from Ribonucleotide Reductase and Photosystem II

radical	g_x	g_y	g_z	g_{ave}[a]
RNR-Tyr°	2.00868	2.00430	2.00203	2.00500
D2-His189gln-TyrD°	2.00832	2.00430	2.00220	2.00494
D2-Tyr190Phe-TyrZ°	2.00750	2.00422	2.00225	2.00466
WT-TyrD°	2.00740	2.00425	2.00205	2.00466
spinach-TyrD°	2.00737	2.00420	2.00208	2.00455

[a] $g_{ave} = (g_x + g_y + g_z)/3$.

D2-His189Gln Mutant. The principal *g* values of the TyrD° in the His189Gln mutant (Figure 1B) are similar to those of the RNR Tyr° spectrum (Table 1). From this we conclude that the glutamine residue either does not hydrogen-bond TyrD° or only does so extremely weakly. The g_x value of TyrD° in the D2-His189Gln was slightly smaller than that of the radical in RNR and may indicate a very weak hydrogen bond by the side-chain amide N-H. This observation is consistent with conventional 9 GHz ENDOR results which show the loss of the 3.1 MHz proton signal identified with the hydrogen bond (Tang et al., 1993). At a given distance and orientation, the side chain of histidine is a stronger hydrogen-bond donor than that of a glutamine (Coulson, 1959). The line widths of the D2-His189Gln tyrosyl radical were slightly larger than those of the wild-type but significantly smaller than that of the radical in RNR. The simplest explanation is that the phenyl ring plane has rotated relative to the β-methylene protons and that the hyperfine coupling is larger. However, this increase in the hyperfine coupling is not apparent in the 9 GHz spectra shown in Figure 2A due to an overlapping signal from a second radical (see below). Nevertheless, the change in hyperfine coupling is also likely to be ob-

scured by the increase in line width due to increase in g-anisotropy.[2]

The superior resolution of HF-EPR is clearly demonstrated by the His189Gln TyrD° spectrum. The spectrum also clearly exhibits another signal between the g_y and g_z components of the tyrosyl spectrum (Figure 1B). This signal is from a chlorophyll radical. Since chlorophyll is a planar aromatic molecule, like the phenolic ring of the tyrosyl radical, the g_z component of the cation radical is expected to be slightly displaced from the free-electron g value (Angstl, 1989). This accounts for relatively high intensity in the g_z region. The extra intensity between g_y and g_z corresponds to the remainder of the chlorophyll signal. It is known that the g anisotropies of the chlorophyll radicals are small. The g values of the bacteriochlorophyll *a* radical are 2.0033, 2.0026, and 2.0022 with an isotropic g value of 2.0027 (Burghaus et al., 1993). The signal observed in the high-field spectra are consistent with these values. The conventional 9 GHz EPR spectrum (Figure 2C) also shows a narrow signal superimposed on the TyrD° spectrum.

D2-Tyr160Phe mutant. Figure 1C is that of TyrZ° from the D2-Tyr160Phe mutant. The principle g values are identical to those of WT-TyrD° and spinach TyrD°. The features of the TyrZ° spectrum at the principal g values appear to be broader than those of the TyrD°. This likely reflects a slightly different orientation of the phenyl ring with respect to the C_β protons. The 9 GHz spectrum of TyrZ° (Figure 2B) is also broader than that of the WT-TyrD°. These observations are consistent with recent detailed EPR studies (Tang et al., 1996; Tommos et al., 1995) which clearly show differences in the C_β proton-ring plane orientations in the two tyrosyl radicals. Unfortunately without resolved hyperfine features, it is difficult to verify the 9 GHz measurements. The major difference between the TyrZ° and WT-TyrD° spectra is the width of the g_x edge. It is clearly much broader than the other two turning points. The shape of the g_x edge was independent of temperature from 3.9 to 21 K (data not shown). From this, we conclude that the broadness is probably not caused by dynamic exchange between sites of different g values and that the shape of the g_x edge must reflect a distribution of magnetically and chemically distinct sites. It was possible to reproduce the line width variation by assuming a g_x value of 2.0075 with a gaussian width of 0.0007 (approximately 30 G, Figure 1C dotted line). The three largest hyperfine tensors (one of the C_β protons and the two protons adjacent to the ring C-O group) as well as the g tensor were included in the calculated spectrum. The hyperfine tensors were from the literature (Tommos et al., 1994; Rigby et al., 1994; Hoganson & Babcock, 1989). The orientations of the tensors were similar to those of TyrD° (Hoganson & Babcock, 1989) and model tyrosyl radicals (Fasanella & Gordy, 1969). This distribution in g_x at 9 GHz amounts to about 1 G and is unlikely to be detectable. As noted above, the 9 GHz spectra of TyrZ° appears to be wider than that of the WT-TyrD° spectrum, but the difference is less than 2 G. Hence, the g_x broadening mechanism is magnetic-field-dependent and cannot be due to either nuclear or electron spin−spin interaction such as to Mn(II) ions. Relaxation measurements also preclude the presence of electron spin−spin interactions (Koulougliotis et al., 1995).

[2] g anisotropy is defined as $|g_x - g_z|$ where $g_x \geq g_y \geq g_z$.

The most straightforward interpretation of the 245 GHz spectra of TyrZ° is that, like TyrD°, it is hydrogen-bonded. On the basis of the broadness of the of g_x feature, we conclude that TyrZ° exists in an electrostatically distributed environment caused by disorder associated with hydrogen bonding. On the average, the hydrogen bonding is similar to that found in the wild-type with an average g_x value of 2.0075. However, in some of the centers the hydrogen bonding is much stronger with the g_x value approaching that of the *in vitro* model studied by Fasnella and Gordy (1969). At the opposite extreme, the g_x value nearly approaches that of the value found for the His189Gln mutant and the RNR Tyr°. At this extreme, the electrostatic stabilization is present but is weak (Un et al., 1995). Only a very small number of centers, if any, have no hydrogen bonds or any other forms of electrostatic stabilization.

Comparison to Other Spectroscopic Results. A recent 9 GHz proton ENDOR study (Tommos et al., 1995) has failed to detect the presence of a hydrogen-bond donor to TyrZ° in the D2-Tyr160Phe mutant. However, using the special triple ENDOR experiment, Tang et al. (1996) detected a broad inverted proton ENDOR signal centered approximately at the same frequency as in WT-TyrD° spectrum. A detailed theoretical treatment of the relationship between the ENDOR and and HF-EPR results is given in the appendix. To summarize, the g_x is essentially determined by the spin-orbit coupling of the singly occupied molecular orbital which describes the unpaired electron and the molecular orbital characterized by nonbonding oxygen electrons. The hydrogen bonding acts as a stabilizing electrostatic perturbation on the nonbonding oxygen electrons. A simple approximation is that nonbonding oxygen electrons are stabilized by the electric dipole of the hydrogen-bond donor and this electrostatic interaction has an approximate $1/r^2$ dependence. By contrast, the ENDOR measures a magnetic dipole-dipole interaction which has a $1/r^3$ dependence. On the basis of this comparison, if we assume that the 3.1 MHz ENDOR signal found in the ENDOR spectrum of TyrD° (Tang et al., 1993, 1996) arises from a proton 1.89 Å away and that the hyperfine coupling is purely dipolar, one would expect the corresponding TyrZ° ENDOR signal to be distributed from 2.0 to 4.5 MHz. Such a broad signal would be difficult to detect. Thus far, it has been assumed that the hydrogen bonding was distributed with respect to donor−acceptor distance. However, the distribution could also result from a variation in the angular orientation of the acceptor and donor (Pimentel & McCellan, 1960). Such an angular variation may result from different orientations of the tyrosyl ring. A detailed analysis of such variations have been recently reported (Warncke et al., 1995) for *in vitro* tyrosyl radicals and has been observed for TyrZ° in the D2-Tyr160Phe mutant (Tommos et al., 1995). A distributed environment about TyrZ° in spinach has been postulated on the basis of variable temperature ENDOR measurements (Mino & Kawamori, 1994). Theoretical g factor calculations indicate that the g_x distribution is also consistent with a variation in either distance or angular orientation or both (data not shown).

A difference FTIR investigation has concluded that TyrZ° is not hydrogen-bonded (Bernard et al., 1995). This conclusion is predicated on the assignment of a peak at 1477 cm^{-1} to the TyrZ° C−O stretch frequency and a peak at 1473 cm^{-1}

to the analogous mode of TyrD°. These frequencies are significantly lower than those found by resonance raman for the tyrosyl radical in ribonucleotide reductase [1498 cm^{-1} (Backes et al., 1989)] and model phenoxy radical [1505 cm^{-1} (Tripathi, 1984)]. A difference FTIR study (Berthomieu, 1995) of *in vitro* tyrosyl radicals and phenoxy radicals has reported C−O stretching frequencies similar to those obtained by resonance raman. It is known that hydrogen-bonding can induce downward shifts in C−O stretch frequencies. Thus, the difference FTIR results on the hydrogen-bonding status of TyrZ° is far from clear.

Origins of the Disordered Environment. What is the underlying cause of the distribution? There are three obvious possibilities. None of these possibilities can be ruled out on the basis of this study. The first possible explanation is that the disorder is induced by the mutation. On the basis of computer models (Ruffle et al., 1992; Svenson et al., 1990, 1991), the Tyr160 mutation is over 30 Å away from TyrZ; hence, it would seem unlikely that the mutation is the source of the disorder. A second possibility is that the observed disorder is inherent. It has been suggested that TyrZ is structurally flexible reflecting its function as a hydrogen atom abstractor (Tommos et al., 1996; Hoganson et al., 1995). Finally, the disorder maybe caused by the manganese depletion. The PSII samples discuss in this paper lack intact manganese clusters. It is known that electron transfer from the water-oxidizing manganese cluster to TyrZ is sensitive to many factors such as the specific S-state of the Mn-cluster (Babcock et al., 1976; Dekker et al., 1984). This may be in part due to a critical balancing of the electrostatic potential in the region between the cluster and the TyrZ (Boussac et al., 1992). Hence, manganese depletion is likely to have significant electrostatic and structural effects which in turn could induce disorder in the hydrogen bonding to TyrZ°. This would clearly be the case if the maganese cluster were proximal to TyrZ (Gilchrist et al., 1995). However, manganese delpletion could have effects over a long distance. Recent electron diffraction studies indicate large scale disruption of the PSII complex upon manganese depletion by Tris washing (Ford, 1995). Regardless of the origins of the disorder about TyrZ°, on the basis of the HF-EPR data, it is clear that, like TyrD°, TyrZ° is hydrogen-bonded and on the average to same extent as TyrD°. Hence, hydrogen bonding by itself does not appear to be the discriminating factor which distinguishes TyrZ° from TyrD° with regards to their stabilities.

ACKNOWLEDGMENT

We thank A. W. Rutherford for helpful discussions. The High Magnetic Field Laboratory is acknowledged for the use of their facilities.

APPENDIX

It can be shown that the spin-orbit contribution to the g_x component of a tyrosyl radical is (Stone, 1963b)

$$\Delta g_x = g_x - g_e \approx \frac{\zeta_0 \varrho_z \varrho_y^*}{\Delta E} = \frac{S_0}{\Delta E} \qquad \text{(A1)}$$

where ζ_O is the spin-orbit coupling of the oxygen (151 cm^{-1}), ρ_z is the oxygen p_z-orbital spin density in the ground state singly occupied molecular orbital, (SOMO) corresponding to a π^* molecular orbital, and ρ_y* is the oxygen p_y-orbital spin density in excited state SOMO corresponding to a nonbonding molecular orbital center on the oxygen; ΔE is the energy difference ground-state SOMO and the excited-state SOMO. If we assume that the hydrogen bond presents a small perturbation to the system, then eq A1 can be expressed

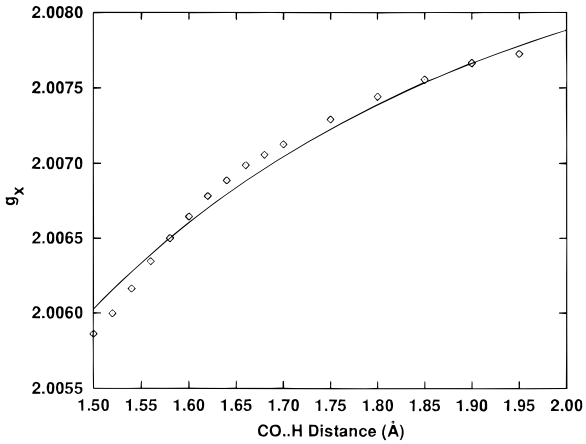

FIGURE 3: Theoretical g_x value as a function of hydrogen-bonding distance for a *p*-methylphenoxy radical which is hydrogen bonded to an acetic acid molecule, calculated using MNDO-PM3 (points) and using a simple electic dipole stabilization model (line; see text for details).

$$\Delta g_x = \frac{S_0 k(r)}{\Delta E + \varphi} \qquad \text{(A2)}$$

where $k(r)$ represents the change in the SOMOs and φ is the difference energy induced by the hydrogen bond on the two states. For modest to weak hydrogen bonds, one can approximate the effect as largely electrostatic and φ is small compared to ΔE. Hence eq A2 can be expanded in terms of φ, which in turn can be expanded in a multipole expansion (i.e., monopole or charge, dipole, quadrapole potential, etc.) and yields

$$\Delta g_x = \frac{S_0 k(r)}{\Delta E}\left(1 - \frac{1}{\Delta E}\left(\frac{C}{r} + \frac{D}{r^2} + ...\right)\right) \qquad \text{(A3)}$$

The expansion has been truncated to include only the potential from electric charges and dipoles. If no charges are present, the *C* term vanishes. At this point, it is assume that the SOMOs are only slightly perturbed [i.e., $k(r) \sim 1$]. As shown in Figure 3, this assumption and the validity of eq A3 is consistent with *g* values calculated using the PM3-MNDO method (Dewar & Theil, 1977; Stewart, 1989) which have recently been shown to yield reliable *g* values for tyrosines (Un et al., 1995). The MNDO calculations were based on the theoretical model of a *p*-methylphenoxy radical/acetic acid hydrogen-bonded pair where distance between the donor (acetic acid) and acceptor (*p*-methylphenoxy radical) has been varied. The data points represent the g_x values as a function of the oxygen to hydrogen distance. No reasonable fit could be obtained using a r^{-2} depedence, however, when the distance was contracted by 0.5 Å. A least-squares fit of the MNDO calculated g_x values yields

$$g_x = 2.0094 - \frac{0.0033}{(r - 0.5)^2} \qquad \text{(A4)}$$

The likely origins of this offset is that the nonbonding oxygen electrons protrude out from the nucleus and their density reaches a maximum at about 0.5 Å.

The frequency of the ENDOR signal arising from a hydrogen-bonding proton is purily determined by magnetic dipole interaction (O'Malley & Babcock, 1987) and will have a r^{-3} dependence. For TyrD°, a 3.1 MHz ENDOR signal has been attributed to the $A_\perp$ component of the proton hyperfine coupling from hydrogen-bond donor. Based on a point dipole approximation and a oxygen spin density of 0.3 (Tommos et al., 1995), the distance from the phenolic oxygen to the proton is about 1.89 Å. If these ENDOR results are compared to the g_x results shown in Figure 3, a distribution in g_x of 0.0007 centered at 2.0075 would correspond to an ENDOR signal centered at 3.1 MHz with a distributed from 2.0 to 4.0 MHz. Hence, the ENDOR signal from the hydrogen-bond donor to TyrZ° is expected to be broad and difficult to observed.

REFERENCES

Angstl, R. (1989) *Chem. Phys. 132*, 435−442.

Babcock, G. T., Blankenship, R. E., & Sauer, K. (1976) *FEBS Lett. 61*, 286−289.

Babcock, G. T., Barry, B. A., Debus, R. J., Hoganson, C. W., Atamian, M., MacIntosh, L., Sithole, I., & Yocum, C. F. (1989) *Biochemistry 28*, 9558−9565.

Bender, C. J., Sahlin M., Babcock, G. T., Barry, B. A., Chandrashekar, T. K., Salowe, S. P., Stubbe, J., Lindström, B., Petersson, L., Ehrenberg, A., & Sjöberg, B.-M. (1989) *J. Am. Chem. Soc. 111*, 8076−8083.

Boussac, A., Sétif, P., & Rutherford, A. W. (1992) *Biochemistry 31*, 1224−1234.

Burghaus O., Plato M., Rohrer, M., Möbius, K., MacMillian, F. & Lubitz, W. (1993) *J. Phys. Chem. 97*, 7639−7647.

Coulson, C. A. (1959) in *Hydrogen Bonding* (Hadzi, D., Ed.) pp 339−360, Pergamon Press, Paris.

Debus, R. J., Barry B. A., Babcock, G. T., & McIntosh L. (1988a) *Proc. Natl. Acad. Sci. U.S.A. 85*, 427−430.

Debus, R. J., Barry, B. A., Sithole, I., Babcock, G. T., & McIntosh, L. (1988b) *Biochemistry 27*, 9071−9074.

Deisenhofer, J., Epp, O., Miki, K., Huber, R., & Michel, H. (1985) *Nature 318*, 618−624.

Dekker, J. P., Plijter, J. J., Ouwehand, L., & van Gorkom, H. J. (1984) *Biochim. Biophys. Acta 767*, 176−179.

Dewar, M. J. S., & Thiel, W. (1977) *J. Am. Chem. Soc. 99*, 4899−4907.

Fasanella, E. L., & Gordy, W. (1969) *Proc. Natl. Acad. Sci. U.S.A. 62*, 299−304.

Ford, C. F., Rosenberg, M. F., Shepherd, F. H., McPhie, P., & Holzenberg, A. (1995) *Micron 26*, 133−140.

Gilchrist, M. L., Bell, J. A., Randall, D. W., & Britt, R. D. (1995) *Proc. Natl. Acad. Sci. U.S.A. 92*, 9545−9549.

Heller, C., & McConnell, H. M. (1960) *J. Chem. Phys. 32*, 1535−1539.

Hoganson, C. W., & Babcock, G. T. (1988) *Biochemistry 27*, 5848−5855.

Koulougliotis, D., Tang, X.-S., Diner, B. A., & Brudvig, G. W. (1995) *Biochemistry 34*, 2850−2856.

Metz, J. G., Nixon, P. J., Rogner, M., Brudvig, G. W., & Diner, B. A. (1989) *Biochemistry 28*, 6960−6969.

Michel, H., & Deisenhofer, J. (1988) *Biochemistry 27*, 1−7.

Mino, H., & Kawamori, A. (1994) *Biochim. Biophys. Acta 1185*, 213−220.

Muller, F., Hopkins, M. A., Coron, N., Grynberg, M., Brunel, L.-C., & Martinez, G. (1989) *Rev. Sci. Instrum. 60*, 3681−3684.

Nordlund, P., & Eklund, H. (1993) *J. Mol. Biol. 232*, 123−164.

O'Malley, P. J., & Babcock, G. T. (1986) *J. Am. Chem. Soc 108*, 3995−4001.

Pimentel, G. C., & McClellan, A. L. (1960) *The Hydrogen Bond*, pp 255−293, W. H. Freeman, San Francisco.

Rigby, S. E. J., Nugent, J. H. A., & O'Malley, P. J. (1994) *Biochemistry 33*, 1734−1742.

Ruffle, S. V., Donnelly, D., Blundell, T. L., & Nugent, J. H. A. (1992) *Photosynth. Res. 34*, 287−300.

Santus et al. (1968) *Photochem. Photobiol. 7*, 341−360.

Schneider, W. G. (1955) *J. Chem. Phys. 23*, 26−30.

Schuster, P. (1976) in *The Hydrogen Bond* (Schuster, P., Zundel G., & Sandorfy, C., Eds.), North-Holland Publishing Co., Amsterdam.

Stewart, J. P. P. (1989) *J. Comput. Chem. 10*, 221−264.

Stone, A. J. (1963a) *Proc. R. Soc. London A 271*, 424−434.

Stone, A. J. (1963b) *Mol. Phys. 6*, 509−515.

Svenson, B., & Strying, S. (1991) *Z. Naturforsch. 46c*, 765−776.

Svenson, B., Vass, I., Cedergren, E., & Strying, S. (1990) *EMBO J. 9*, 2051−2059.

Tang, X.-S., Chisholm, D. A., Dismukes, G. C., Brudvig, G. W., & Diner, B. A. (1993) *Biochemistry 32*, 13742−13748.

Tang, X.-S., Zheng, M., Chisholm, D. A., Dismukes, G. C., & Diner, B. A. (1996) *Biochemistry* (in press).

Tommos, C., Davidsson, L., Svensson, B., Madsen, C., Vermass, W. F. J., & Styring, S. (1993) *Biochemistry 32*, 5436−5441.

Tommos, C., Madsen, C., Styring, S., & Vermass, W. F. J. (1996) *Biochemistry 33*, 11805−11813.

Tommos, C., Tang, X.-S, Warncke, K., Hoganson, C. W., Styring, S., McCracken, J., Diner, B. A., & Babcock, G. T. (1995) *J. Am. Chem. Soc. 117*, 10325−10335.

Un, S., Brunel, L.-C., Brill, T., Zimmermann, J.-L., & Rutherford, A. W. (1994) *Proc. Natl. Acad. Sci. U.S.A. 91*, 5262−5266.

Un, S., Atta, M., Fontecave, M., & Rutherford, A. W. (1995) *J. Am. Chem. Soc. 117*, 10713−10719.

Vermaas, W. F. J., Rutherford, A. W., & Hansson, O. (1988) *Proc. Natl. Acad. Sci. U.S.A. 85*, 8477−8481.

Warncke, K., Babcock, G. T., & McCracken, J. (1994) *J. Am. Chem. Soc. 116*, 7332−7340.

Warncke, K., Babcock, G. T., & McCracken, J. (1995a) *J. Am. Chem. Soc. 116*, 7332−7340.

Warncke, K., & McCracken, J. (1995b) *J. Chem. Phys.* (in press).

BI9523769